Click synthesis of symmetric bis-triazol ligands and full characterisation of their copper(II)-complexes

Article *in* New Journal of Chemistry · December 2013

DOI: 10.1039/C3NJ00570D

CITATIONS
9

READS
82

8 authors, including:

Mustapha Allali
High Institute of nursing and health techniques-Fes/ ISPITS-fes
24 PUBLICATIONS **222** CITATIONS
SEE PROFILE

Marc Beley
University of Lorraine
83 PUBLICATIONS **2,674** CITATIONS
SEE PROFILE

Wenger Emmanuel
University of Lorraine
100 PUBLICATIONS **313** CITATIONS
SEE PROFILE

Maxime Bernard
University of Strasbourg
21 PUBLICATIONS **552** CITATIONS
SEE PROFILE

NJC

PAPER

View Article Online
View Journal | View Issue

Cite this: *New J. Chem.*, 2014, **38**, 419

Click synthesis of symmetric bis-triazol ligands and full characterisation of their copper(II)-complexes†

Zakia Benkhellat,[a] Mustapha Allali,[a] Marc Beley,[a] Emmanuel Wenger,[b] Maxime Bernard,[c] Nathalie Parizel,[c] Katalin Selmeczi[a] and Jean-Pierre Joly*[a]

Received (in Montpellier, France) 28th May 2013,
Accepted 31st October 2013

DOI: 10.1039/c3nj00570d

www.rsc.org/njc

Eight novel ligands were prepared from a known symmetric diaza-18-crown-6 (cyclic ligand) and two commercial *N*,*N*′-dimethyl-alkyl diamines (acyclic ligands) *via* the Cu(I)-catalyzed Huisgen dipolar cycloaddition. All C_2-symmetric isolated ligands readily formed stable crystalline 1 : 1-copper(II) complexes with cupric perchlorate. Their structural, electrochemical and physico-chemical properties were fully investigated with the help of X-ray diffraction, cyclic voltammetry, FT-IR, UV-visible, and electron paramagnetic resonance (EPR) spectroscopies. Planar – or nearly planar – arrangement of the two N3-triazole nitrogens and the two tertiary amine pivot nitrogens was found in one single four-coordinated species, in four five-coordinated species, and three six-coordinated species, with one or two solvent molecule(s), or two oxygen atoms of the crown ether, occupying the axial position(s) in the solid sate. The electron-donating or electron-withdrawing effect of the N1-substituent on the triazol was found to influence the Cu(II)/Cu(I) redox potential of all studied complexes in DMF. The EPR-spectrum of cyclic complexes in frozen DMF at 100 K exhibited two mononuclear species, one of them likely promoting the formation of dinuclear species as a minor component, whereas most acyclic complex spectra were quite similar.

Introduction

Copper is second to iron in its prevalence in redox-active metalloproteins,[1] mainly as a cofactor of numerous enzymes (*e.g.* cytochrome-*c* oxidase,[2] copper-thionein,[3] ceruloplasmin,[4] dopamine-β-mono-oxygenase,[5] galactose oxidase,[6] and many others). Copper is believed to play a significant role in the CNS-development of mammalians, too.[7] Although this metal is of critical importance in numerous biochemical processes, free copper (*i.e.* uncomplexed Cu^{+} or Cu^{2+} cations) is actually cytotoxic.[8,9] Therefore, versatile ligands of copper ions receive growing interest from the chemist community as models of natural enzymes[10,11] (such as superoxide dismutase mimetics[12]), but also as new HIV-antiviral agents,[13] anti-cancer agents,[14,15] receptor-mediated tumour imaging agents,[16,17] and catalysts of organic reactions.[18] Functionalized 1,4-disubstituted 1,2,3-triazole units are versatile ligands offering several donor sites or act as bridging ligands for copper and some other rare transition metal coordination too.[19–27] A large array of mono, bi, tri-, and polydentate ligands incorporating 1,4-disubstituted-1,2,3-triazoles has been synthesized since 2007.[28–31] Moreover, the Cu(I)-catalyzed version of the [3+2] Huisgen[32–35] azide–alkyne cycloaddition (*i.e.* the CuAAC 'click reaction')[36–38] was used to synthesize ligands endowed with good complexing properties towards zinc, lead, nickel, and ammonium too.[39–43] In the meantime, this powerful synthetic approach was extended to the linkage of cyclodextrines to various organic azides.[44] We reported the synthesis of a new C_2-symmetric macrocyclic ligand (hereafter **L1**, a pendant armed 18-crown-2-diaza-4-ether) endowed with good complexing properties towards copper,[45] nickel and zinc cations, too.

Solid-state structures revealed two different coordination modes, one symmetrical for Cu(II), quite isomorphous with the Ni(II)-analogue, *versus* one asymmetric for Zn(II), which were further investigated *via* molecular modelling. These results will be discussed elsewhere.[46] During the course of this work,

[a] *SRSMC UMR 7565 CNRS – Université de Lorraine, Faculté des Sciences, BP 70239, F-54506 Vandœuvre-lès-Nancy cedex, France. E-mail: jean-pierre.joly@sucres.uhp-nancy.fr*
[b] *CRM_2, UMR 7036 CNRS – Université de Lorraine, Faculté des Sciences, BP 70239, F-54506 Vandœuvre-lès-Nancy cedex, France*
[c] *TGE Réseau National de RPE interdisciplinaire, FR-3443, Institut de Chimie, UMR 7177 CNRS – Université de Strasbourg, 4 rue Blaise Pascal, CS 90032, 67081 Strasbourg cedex, France*

† Electronic supplementary information (ESI) available: Synthesis and full characterisation of **L2–9** ligands including ES-HRMS^{+} spectra of all reported complexes; EPR spectra (Q-band at 100 K) of [Cu**L9**(ClO_4)]ClO_4 (**S1**) and [Cu**L4**](ClO_4)$_2$ (**S2**) complexes in PDF format; low resolution crystallographic data & structure refinement parameters of the [Cu**L9**(ClO_4)](ClO_4) complex and **T1** in CIF format. CCDC 853231, 851236–851242, 854682. For ESI and crystallographic data in CIF or other electronic format see DOI: 10.1039/c3nj00570d

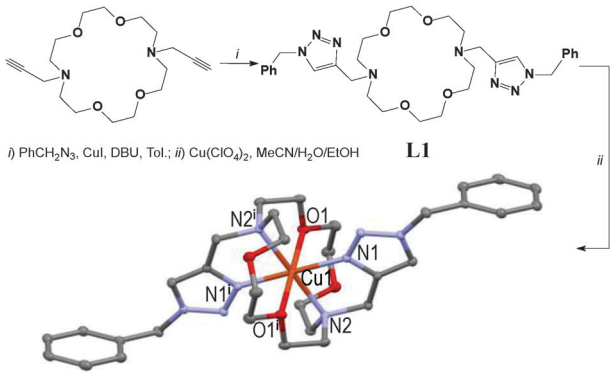

Fig. 1 Two-step synthesis of the [Cu**L1**](ClO$_4$)$_2$ centro-symmetric complex in 31% overall yield (symmetry code: (i) $1-x, 1-y, 1-z$).[45]

tetradentate ligands from a *N*,*N*′-dimethyl-1,2-diaminoethane synthesized *via* click chemistry were reported and their complexes with Mn^{2+}, Ni^{2+}, Zn^{2+}, and Fe^{2+} generated. Among them, their Mn^{2+}-complexes displayed interesting catalytic activities for the epoxidation of various terminal olefins with peracetic acid.[18] We describe herein the 'click' syntheses of two series of new macrocyclic and acyclic ligands *via* the Cu(I)-catalyzed version of the Huisgen reaction between a terminal acetylene and an organic azide. The Cu(II)-complexes of these ligands were isolated (as their perchlorate salts) and characterised *via* different techniques: elemental analysis, FT-IR, UV-visible and EPR spectroscopies, HRMS$^+$, high resolution X-ray diffraction (for seven over eight complexes), and cyclic voltammetry.

Results and discussion

Synthesis and characterisation of ligands

Cyclic ligands **L2–4** were click-generated in good to fair yields from known *N*,*N*′-dipropargyl-diaza crown A[47] and readily available aryl-azides (*i.e.* Scheme 1, general procedure I and ESI†).[48–50]

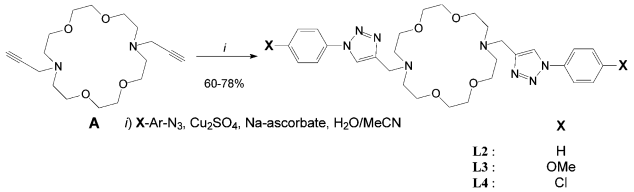

Scheme 1 Synthesis of cyclic ligands **L2–4** from diaza-crown ether A.

Acyclic ligands **L5–9** were isolated in fair to good yields using a slight modification of the one-pot method reported by Yan *et al.*[51] from commercial secondary bis-*N*-methyl amines B and C (*i.e.* general procedure II and ESI†).

The tedious isolation of *N*,*N*′-dipropargyl bis-tertiary amine intermediates (after step i) did not improve overall yields (Scheme 2). Some ligands (*e.g.* **L7** & **L8**) have to be chromatographed twice over silica and/or neutral alumina to ensure sufficient purity and unambiguous characterization. All ligand structures were unambiguously ascertained by ^{1}H & ^{13}C-NMR, FT-IR, and ES$^+$-HRMS. ^{1}H-NMR spectra of all ligands exhibit the expected time-averaged 2-fold symmetry and the characteristic aromatic singlet between 7.5 and 8.0 ppm for the two isochronous triazol protons at the NMR time scale ($CDCl_3$, 298 K).

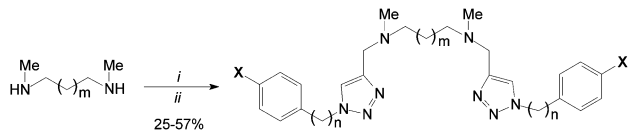

	m	n	X
L5 :	0	1	H
L6 :	1	1	H
L7 :	1	0	H
L8 :	1	0	OMe
L9 :	1	0	Cl

Scheme 2 One-pot synthesis of ligands **L5–9** *via* the Cu(I)-catalyzed Huisgen reaction.

Table 1 Crystal data & structure refinement parameters of cyclic Cu(II)-complexes from ligands **L2–4** with respect to **L1**[45]

Complexes	[Cu**L1**](ClO$_4$)$_2$	[Cu**L2**](ClO$_4$)$_2$	[Cu**L3**](ClO$_4$)$_2$	[Cu**L4**](ClO$_4$)$_2$, DMF
Empirical formula	$CuC_{32}H_{44}Cl_2N_8O_{12}$	$CuC_{30}H_{40}Cl_2N_8O_{12}$	$CuC_{32}H_{44}Cl_2N_8O_{14}$	$CuC_{33}H_{45}Cl_4N_9O_{13}$
Formula weight	867.19	839.15	899.20	981.13
Colour	Light blue	Blue-green	Dark green	Malachite-green
Cryst. size [mm]	0.32 × 0.18 × 0.14	0.12 × 0.10 × 0.08	0.31 × 0.19 × 0.11	0.21 × 0.14 × 0.10
Crystal system	Triclinic	Triclinic	Triclinic	Monoclinic
a [Å]	9.1849(15)	9.390(5)	9.383(5)	26.3848(4)
b [Å]	9.2931(8)	10.293(5)	10.299(8)	18.7279(3)
c [Å]	11.8913(12)	10.426(5)	11.300(9)	27.6457(6)
α [deg]	98.876(4)	101.979(5)	70.19(4)	90.00
β [deg]	108.784(5)	108.296(5)	66.08(3)	143.2590(10)
γ [deg]	105.480(6)	106.798(5)	73.30(5)	90.00
V [Å^3]	893.40(19)	865.2(7)	924.7(1)	8171.8(3)
Space group	$P\bar{1}$	$P\bar{1}$	$P\bar{1}$	$P2_1/c$
Z	1	1	1	8
ρ_{calcd} [g cm^{-3}]	1.612	1.618	1.615	1.595
Temp. [K]	110(2)	110(2)	100(2)	100(2)
R/w*R*	0.0286/0.0696	0.0249/0.0661	0.0344/0.0806	0.0400/0.0947
GOF	1.041	1.047	1.062	1.025
CCDC	854682	853231	851236	851237

Further information about the isolation and full characterisation of ligands **L2–9** is provided in the ESI.†

Crystallographic characterization

Suitable X-ray diffraction monocrystals of 1 : 1 Cu(II)-complexes were isolated from ligands **L2–8** and $Cu(ClO_4)_2$ hexahydrate in the presence of acetonitrile and dimethylformamide (traces) in fair to excellent yield within a week (see general procedure III and ESI†). Their crystallographic data are summarised in Tables 1 and 3.

Cyclic ligands. Selected bond distances and angles of cyclic Cu(II)-complexes of ligands **L2–4** are summarised in Table 2 with respect to **L1**.[45]

The three first cyclic Cu(II)-complexes, *i.e.* [Cu**L1–3**]$(ClO_4)_2$, crystallised in the triclinic space group $P\bar{1}$ as their perchlorate salts, with the central Cu-atom lying on the the inversion centre.

However, the new [Cu**L2**]$(ClO_4)_2$ centro-symmetric complex (see Fig. 2) is quite different from [Cu**L1**]$(ClO_4)_2$,[45] but very similar to [Cu**L3**]$(ClO_4)_2$ (see Fig. 3) with close bond distances and bond angles. It is noteworthy that the N1–Cu1–O1 angle was significantly smaller in [Cu**L1**]$(ClO_4)_2$ (*i.e.* 84.7°) than in [Cu**L2**]$(ClO_4)_2$ and [Cu**L3**]$(ClO_4)_2$ (~87.3°).

Here again, the hexacoordinated Cu(II)-cation lies on the inversion centre in the basal plane formed by the four N-atoms and O1 occupies the axial position in the centro-symmetric complex (see Fig. 3). Strained 5-membered cycles (*i.e.* N1–Cu1–N2 and O1–Cu1–N2) induce bond angles diminution and a slightly distorted six-coordinated octahedral geometry. The Cu1–O1 distances fall in the range of 2.536 ± 0.011 Å in accordance with the Jahn–Teller effect.[52] Replacement of the EDG-methoxy group by the EWG-chlorine atom in **L4** (all else being equal) led to a completely different solid-state structure.

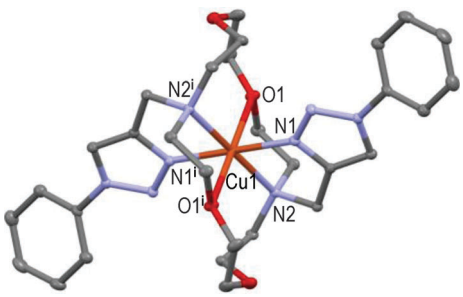

Fig. 2 Molecular structure of [Cu**L2**]$(ClO_4)_2$ showing the hetero-atom numbering and the thermal ellipsoids at 50% probability (H-atoms and non-coordinating anions omitted for clarity; symmetry code: (i) −*x*, −*y*, −*z*).

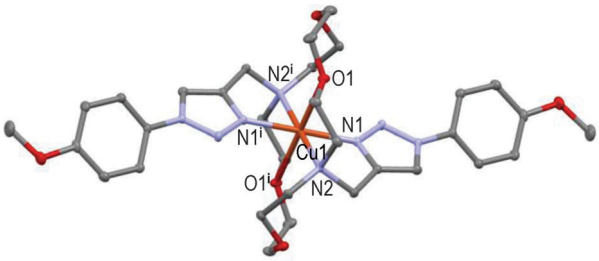

Fig. 3 Molecular structure of [Cu**L3**]$(ClO_4)_2$ showing the hetero-atom numbering and the thermal ellipsoids at 50% probability (H-atoms and non-coordinating anions omitted for clarity; symmetry code: (i) −*x*, −*y*, 1 − *z*).

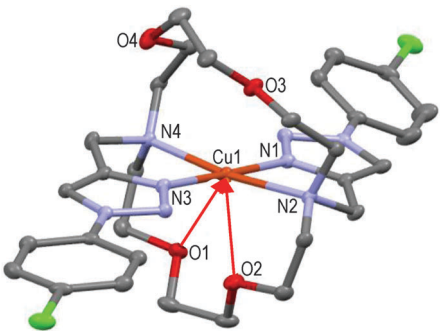

Fig. 4 Molecular structure of one of the two independent [Cu**L4**]$(ClO_4)_2$ molecules present in the asymmetric unit showing the hetero-atom numbering and the thermal ellipsoids at 50% probability (H-atoms and non-coordinating anions omitted for clarity).

The tetracoordinated Cu(II) cation lies above (~0.1 Å) the basal plane formed by N1–N2–N3–N4 in a quite distorted geometry (N1–Cu1–N2 = 80.8°, N3–Cu1–N4 = 83.1°); lone pairs of O1 and O2 oxygen atoms point towards the copper cation (*i.e.* red arrows: Cu1–O1 ~2.71 Å, Cu1–O2 ~2.79 Å), O3 and O4 atoms being too far to interfere with the metal ion (see Fig. 4).

Acyclic ligand Cu(II)-complexes. Their crystallographic data are summarised in Table 3.

Selected bond distances and angles of acyclic Cu(II)-complexes from ligands **L5–9** are summarised in Table 4.

Unfortunately, structure of the [Cu**L9**(ClO_4)](ClO_4) complex could not be fully resolved in spite of numerous attempts under different conditions. However, its low resolution structure is given in Fig. 5 for comparison purposes in the acyclic series.

The above 1 : 1-complex is 'roughly' symmetric, with the pentacoordinated Cu(II)-ion lying approximately 0.1 Å over the

Table 2 Selected bond distances (Å) and bond angles (°) in solid state structures of cyclic Cu(II)-complexes from **L2–4** with respect to **L1**

	Bond distances (Å)				Bond angles (°)			
Cyclic complexes	Cu1–N1	Cu1–N2	Cu1–N3	Cu1–N4	N1–Cu1–N2	N2–Cu1–N3	N3–Cu1–N4	N1–Cu1–N4
[Cu**L1**]$^{2+}$	1.988	2.114	—	—	80.7	99.3[a]	—	—
[Cu**L2**]$^{2+}$	2.015	2.096	—	—	81.1	98.9[a]	—	—
[Cu**L3**]$^{2+}$	2.011	2.107	—	—	81.3	98.7[a]	—	—
[Cu**L4**]$^{2+}$ [b]	1.950	2.178	1.941	2.166	80.4	101.3	82.9	95.2

[a] *i.e.* N2–Cu–N1^{i} bond angle, N1^{i} and N3 being equivalent *via* the inversion centre *cf.* Fig. 1–3. [b] Mean values of two independent molecules.

Table 3 Crystal data & structure refinement parameters of acyclic Cu(II)-complexes from ligands **L5–8**

Complexes	[Cu**L5**(MeCN)](ClO$_4$)$_2$	[Cu**L6**(ClO$_4$)](ClO$_4$)	[Cu**L7**(MeCN)](ClO$_4$)$_2$	[Cu**L8**(DMF)$_2$](ClO$_4$)$_2$
Empirical formula	$CuC_{26}H_{33}Cl_2N_9O_8$	$CuC_{25}H_{32}Cl_2N_8O_8$	$CuC_{25}H_{31}Cl_2N_9O_8$	$CuC_{31}H_{46}Cl_2N_{10}O_{12}$
Formula weight	734.06	707.04	720.03	885.22
Colour	Deep blue	Purple	Deep purple	Blue
Cryst. size [mm]	0.30 × 0.20 × 0.12	0.20 × 0.15 × 0.13	0.20 × 0.15 × 0.10	0.31 × 0.24 × 0.11
Crystal system	Triclinic	Orthorhombic	Triclinic	Triclinic
a [Å]	10.573(4)	14.8356(4)	13.8278(5)	10.806(3)
b [Å]	10.596(4)	25.4907(6)	14.1824(5)	12.898(3)
c [Å]	16.788(5)	8.1556(2)	16.0830(7)	14.296(3)
α [deg]	73.602(4)	90.00	89.792(4)	80.45(1)
β [deg]	79.087(5)	90.00	78.263(4)	85.53(1)
γ [deg]	60.693(3)	90.00	87.476(2)	73.19(1)
V [Å^3]	1570.4(11)	3084.2(13)	3085.1(2)	1880.0(8)
Space group	$P\bar{1}$	$Cmc2_1$[a]	$P\bar{1}$	$P\bar{1}$
Z	2	4	4	2
ρ_{calcd} [g cm^{-3}]	1.552	1.523	1.550	1.564
Temp. [K]	100(2)	100(2)	100(2)	100(2)
R/wR	0.0347/0.0795	0.0465/0.1239	0.0848/0.18344	0.0474/0.1067
GOF	1.052	1.192	1.199	1.063
CCDC	851241	851242	851238	851239

[a] Flack value = 0.4745(8).

Table 4 Selected bond distances (Å) and bond angles (°) in solid state structures of acyclic Cu(II)-complexes from ligands **L5–9**

	Bond distances (Å)				Bond angles (°)			
Acyclic complexes	Cu–N1	Cu–N2	Cu–N3	Cu–N4	N1–Cu–N2	N2–Cu–N3	N3–Cu–N4	N1–Cu–N4
[Cu**L5**(MeCN)]$^{2+}$	1.984	2.036	2.036	1.962	81.5	86.8	82.4	103.3
[Cu**L6**(ClO$_4$)]$^+$	1.961	2.046	—	—	82.5	96.7[a]	—	—
[Cu**L7**(MeCN)]$^{2+}$[b]	1.985	2.055	2.058	1.975	81.7	96.6	82.0	98.6
[Cu**L8**(DMF)$_2$]$^{2+}$	2.002	2.066	2.052	1.986	82.5	95.9	82.1	99.5
[Cu**L9**(ClO$_4$)]$^+$[c]	1.99–	2.07–	2.08–	1.97–	82.–	96.–	83.–	99.–

[a] *i.e.* N2–Cu–N2^{iii} bond angle, N2^{iii} and N3 being equivalent by mirror symmetry *cf.* Fig. 7. [b] Mean values of two independent molecules. [c] See ESI for the low resolution CIF file and selected crystal data (T1).

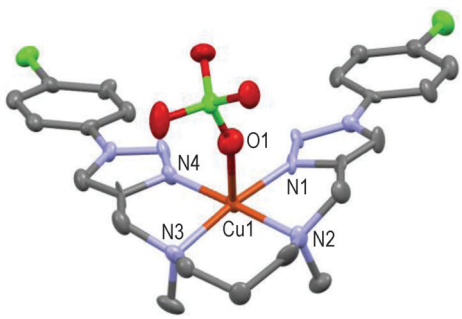

Fig. 5 Low resolution molecular structure of [Cu**L9**(ClO$_4$)](ClO$_4$) showing the hetero-atom numbering and the thermal ellipsoids at 50% probability (H-atoms and non-coordinating anions omitted for clarity).

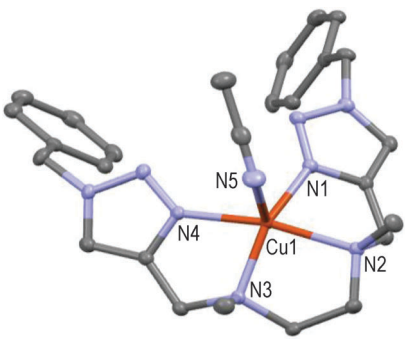

Fig. 6 Molecular structure of [Cu**L5**(MeCN)](ClO$_4$)$_2$ showing the hetero-atom numbering and the thermal ellipsoids at 50% probability (H-atoms and non-coordinating anions omitted for clarity).

basal plane formed by N1–N2–N3–N4 in a square-pyramidal geometry; one oxygen atom of the perchlorate anion occupies the axial position (Cu1–O1 ~2.37 Å, N1–Cu1–O1 ~94.3°) as the 5th ligand. Thanks to the 6-membered cycle (N2–Cu1–N3) the resulting structure is more relaxed than that of [Cu**L5**(MeCN)]$^{2+}$ as illustrated in Fig. 6.

This mono-solvated complex is not endowed with true symmetry; N1–N2–N3–N4 forms the basal plane and N5 of one acetonitrile molecule occupies the axial position (Cu1–N5 = 2.246 Å and N1–Cu1–N5 = 97.7°) as the 5th ligand in a distorted square pyramidal geometry. Strained 5-membered cycles (*i.e.* N1–Cu1–N2, N2–Cu1–N3, N3–Cu1–N4) induce bond angles diminution in comparison to [Cu**L9**(ClO$_4$)]$^+$ (see Fig. 5) and a significant repulsion of the pentacoordinated Cu-atom above the basal plane (~0.34 Å). An extra carbon atom between N2 and N3 atoms in ligand **L6** led to a completely different structure for the resulting Cu(II)-complex (see Fig. 7).

Thanks to the 6-membered cycle (*i.e.* –N2–Cu1–N2^{iii}–(CH$_2$)$_3$–) the mirror-symmetric [Cu**L6**(ClO$_4$)]$^+$ structure is more relaxed

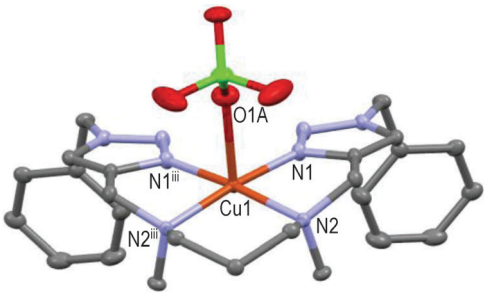

Fig. 7 Molecular structure of [Cu**L6**(ClO_4)]ClO_4 showing the hetero-atom numbering and the thermal ellipsoids at 50% probability (H-atoms and non-coordinating anions omitted for clarity; symmetry code: (iii) $-x, y, z$).

than those of $[Cu\mathbf{L5}(MeCN)]^{2+}$. The pentacoordinated Cu(II)-ion lies approximately 0.13 Å over the basal plane formed by N1–N2–$N2^{iii}$–$N1^{iii}$ in a square-pyramidal geometry; O1A of one perchlorate anion occupies the axial position (Cu1–O1A ~2.42 Å) as the 5th ligand. Interestingly, direct attachment of the phenyl group to the triazole moieties (all else being equal) induced a different coordination of Cu(II) by ligand **L7**.

The resulting 1 : 1-complex is here only approximately symmetric, the pentacoordinated Cu(II) cation at 0.07 Å centered over the basal plane formed by N1–N2–N3–N4 in a square-pyramidal geometry (see Fig. 8); N5 of one acetonitrile molecule occupies the axial position (N1–Cu1–N5 = 92.1°) as the 5th ligand. Lastly, the bis-solvated 1 : 1-complex formed from the *para*-methoxy-phenyl-substituted **L8** ligand and Cu(II) in the presence of DMF is quite different and unique in the acyclic series (see Fig. 9).

The hexacoordinated Cu(II) cation lies in the basal plane formed by N1–N2–N3–N4 in a distorted octahedral geometry; O1A and O1B of two DMF molecules occupy the axial positions respectively 2.367 Å and 2.548 Å apart from the copper cation, which fall in the range of reported values.[53,54] This structure can be compared to that of the $[Cu\mathbf{L3}](ClO_4)_2$ complex (Fig. 3) in the cyclic series. In summary, ligands **L2–9** readily form stable 1 : 1-Cu(II) complexes in the presence of $Cu(ClO_4)_2$ in solution. Three different geometries (*i.e.* tetra-, penta-, and hexa-coordination)

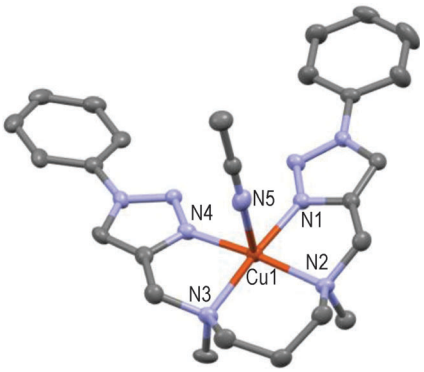

Fig. 8 Molecular structure of one of the two independent [Cu**L7**(MeCN)]-$(ClO_4)_2$ molecules present in the asymmetric unit showing the hetero-atom numbering and the thermal ellipsoids at 50% probability (H-atoms and non-coordinating anions omitted for clarity).

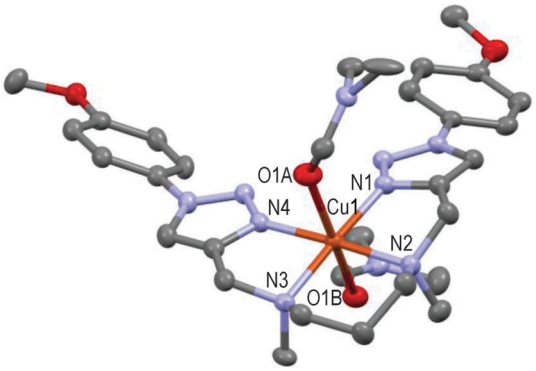

Fig. 9 Molecular structure of $[Cu\mathbf{L8}(DMF)_2](ClO_4)_2$ showing the hetero-atom numbering and the thermal ellipsoids at 50% probability (H-atoms and non-coordinating anions omitted for clarity).

were observed in the solid state with respect to the nature of the ligand (cyclic *vs.* acyclic) and the nature of the substituent on the triazoles. One or two solvent molecule(s), or one perchlorate anion, act(s) eventually as axial ligand(s) in the more open acyclic series to complete the coordination sphere.

Electrochemical studies

It is noteworthy that the formation of Cu^o-species occurs at about −1.5 V as an irreversible process and that the formation of a Cu(III)-complex was not detected before the solvent oxidation which started at +1.5 V under our experimental conditions. Therefore, we studied the electrochemical behavior starting potential at +0.2 V towards negative values and kept the potential range between −0.4 and +0.8 V to avoid the irreversible formation of Cu^o and the oxidation of the solvent throughout the present study. Table 5 summarizes the electrochemical results corresponding to the first cathodic peak (1st scan towards negative potential at three increasing scan rates) which was assigned to the reduction of the initial and stable geometric form, *i.e.* Cu(II)st to Cu(I). A reductive-controlled potential coulometry realized below the 1st cathodic peak at −0.4 V showed that the total quantity of electricity exchanged corresponds to one electron per mole of the copper complex.

Table 5 Electrochemical data for the 1st cathodic peak assigned to the reduction of Cu(II)st to Cu(I): Epc (mV *vs.* SCE) and Ipc (μA) in Cu(II)-complexes from ligands **L1–9** at three different scan rates

	Cyclic ligands				Acyclic ligands				
	L1	**L2**	**L3**	**L4**	**L5**	**L6**	**L7**	**L8**	**L9**
Epc 25 mV s^{-1}	−10	+30	+30	+60	−10	−25	−50	−21	+35
Ipc 25 mV s^{-1}	−11	−12	−11	−11	−12	−10	−11	−11	−11
Epc 100 mV s^{-1}	−20	+10	+20	+45	−30	−45	−65	−50	−10
Ipc 100 mV s^{-1}	−22	−24	−22	−22	−24	−20	−21	−22	−22
Epc 500 mV s^{-1}	−40	0	+5	+40	−50	−100	−120	−90	−15
Ipc 500 mV s^{-1}	−49	−52	−50	−50	−54	−45	−49	−50	−50

First cathodic peak reduction potential (*i.e.* Epc) analyses revealed the ligand-based electrochemical behavior of all present complexes. On the one hand, the donor or withdrawing effect of the *para*-substituent on the phenyl ring was found to influence more or less the reduction potential of the complexes. For instance, $[Cu\mathbf{L4}]^{2+}$ and $[Cu\mathbf{L9}(ClO_4)]^{+}$ display a Cu(II)st → Cu(I) redox potential at more positive values than the corresponding unsubstituted complexes in cyclic and acyclic series, *i.e.* $[Cu\mathbf{L2}]^{2+}$ and $[Cu\mathbf{L7}(MeCN)]^{2+}$, respectively. Thus, the electron withdrawing effect of the chlorine substituent decreases the electronic density around the cupric ion and induces a positive shift in the reduction potential from Cu(II) to Cu(I). In the cyclic series (*e.g.* X = H, $[Cu\mathbf{L2}]^{2+}$), the *N*-triazole doublets are likely more delocalized than in $[Cu\mathbf{L1}]^{2+}$ (no possible π-conjugation). Accordingly, the donor effect of the triazole moiety significantly increases the electron density around the metal in $[Cu\mathbf{L1}]^{2+}$ with a negative shift (*ca.* 35 mV) of the Epc value in comparison to $[Cu\mathbf{L2}]^{2+}$. In the acyclic series, the reduction potential of $[Cu\mathbf{L7}(MeCN)]^{2+}$ (m = 1, n = 0, X = H), including one acetonitrile molecule as the axial ligand, is more negative than those of $[Cu\mathbf{L8}(DMF)_2]^{2+}$ (m = 1, n = 0, X = OMe) and $[Cu\mathbf{L6}(ClO_4)]^{+}$ (m = 1, n = 1, X = H), the donor effect of the acetonitrile ligand being obviously stronger than the remote methoxy effect in $[Cu\mathbf{L8}(DMF)_2]^{2+}$. The mild donor effect of the methoxy group on the phenyl also induces the almost same reduction potentials (Epc ∼ 30 mV) in $[Cu\mathbf{L2}]^{2+}$ (X = H) as in $[Cu\mathbf{L3}]^{2+}$ (X = OMe). On the other hand, the reduction of Cu(II)st to Cu(I) is easier in $[Cu\mathbf{L5}(MeCN)]^{2+}$ than in $[Cu\mathbf{L6}(ClO_4)]^{+}$. We attributed the higher measured Epc to the relative destabilization of Cu(II) in the more distorted geometry of $[Cu\mathbf{L5}(MeCN)](ClO_4)_2$ (m = 0) *vs.* $[Cu\mathbf{L6}(ClO_4)]ClO_4$ (m = 1).[56] It is well-known that there are important differences in geometrical requirements for coordination of Cu(I) in comparison to Cu(II) that produce interesting dynamic processes in solution. Divalent copper preferentially forms stable hexacoordinated, or square pyramidal, complexes whereas the monovalent state induces tetrahedral coordination. The occurrence of structural rearrangements in the first coordination shell of Cu(II) to Cu(I) in the redox mechanism has been largely investigated because many processes in bioinorganic chemistry, catalysis, and supramolecular chemistry involve electron-transfer steps in copper complexes.[1] As illustrated in Table 5, the 1st reduction peak potential of each complex, *i.e.* Epc, depends on the scan rate since its value increases as the scan rate decreases. This behaviour suggests that the reduction of the initial and stable geometric form Cu(II)st gives intermediate metastable species, *i.e.* Cu(I)met, which can rearrange into a more stable form, *i.e.* Cu(I)st, according to a two-step $E_{red}C_{red}$ reaction, that is:

$$E_{red}\ \text{step:}\quad \text{Cu(II)st} + \bar{e} \leftrightarrows \text{Cu(I)met}$$

followed by a

$$C_{red}\ \text{step:}\quad \text{Cu(I)met} \rightarrow \text{Cu(I)st}$$

In an attempt to characterize the re-oxidation steps of Cu(I)mt and Cu(I)st, CV between −0.4 and +0.8 V was performed.

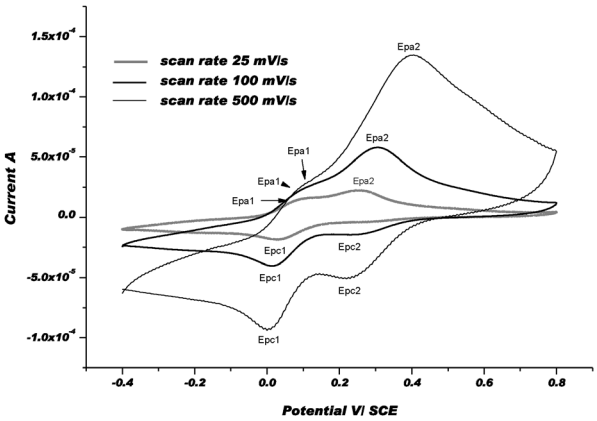

Fig. 10 CVs of $[Cu\mathbf{L4}]^{2+}$at 3 different scan rates: 25, 100, and 500 mV s^{-1} in Ar-purged DMF with 0.1 M Bu_4NPF_6 as a supporting electrolyte at rt.

The second scan was selected as a typical CV. The electrochemical behavior of $[Cu\mathbf{L4}](ClO_4)_2$ is presented below (Fig. 10) as a relevant example in the cyclic series.

The positive part of CVs obviously displays two oxidation waves: a 1st wave, *i.e.* Epa1, which appears at about +90 mV and a second one, *i.e.* Epa2, at about +300 mV under our experimental conditions. After the 1st electrochemical step between +0.2 and −0.4 V (E_{red}), especially when the scan rate was slow, the chemical step, *i.e.* Cu(I)met → Cu(I)st, became more complete and the Cu(I)st/Cu(I)met ratio was much higher. For that reason, the 1st wave was assigned to the re-oxidation of Cu(I)st to Cu(II)met1 and the 2nd one to the formation of Cu(II)met2 from Cu(I)met. Thus, we postulated that the re-oxidation of Cu(I)-complexes, *i.e.* Cu(I)met and Cu(I)st, produces metastable Cu(II)-species *via* an electron transfer followed by a chemical step that is referred to as the so-called $E_{ox}C_{ox}$ mechanism. Indeed, after changing the scan direction at 800 mV, and since 1st reduction potential, *i.e.* Epc1, remains the same as in the first scan (*i.e.* Epc), we assumed that Cu(II)met1 and/or Cu(II)met2 relax to the initial and more stable form Cu(II)st. As shown in the CVs, the chemical rearrangement C_{ox} is complete at 25 mV s^{-1}. At faster scan rates, this chemical rearrangement is not complete and another reduction wave, *i.e.* Epc2, appears at about 0.2 V more anodic potential *vs.* Epc1. As described earlier, we postulate that the metastable forms of Cu(I) and Cu(II)-complexes should be coordinated by solvent molecule(s).[54] Fig. 11 displays the CVs obtained with $[Cu\mathbf{L8}(DMF)_2](ClO_4)_2$ as a relevant complex in the acyclic series. For each scan rate, the CVs in the positive part display three re-oxidation waves. The 1st wave, *i.e.* Epa1 at a potential of about 110 mV *vs.* SCE, was attributed to the re-oxidation of Cu(I)st to Cu(II)met1. The two other waves, corresponding to Epa2 and Epa3, were ascribed to the re-oxidation of metastable Cu(I)met_1 and Cu(I)met_2 species formed by the reduction of Cu(II)st during the 1st scan.

However, reversing the scan direction at 800 mV induces only one reduction peak which was clearly observed at 25 and 100 mV s^{-1} (*i.e.* Epc1). Moreover, another reduction step occurred at about +0.25 V, *i.e.* Epc2, at 500 mV s^{-1} with a very low current intensity. For each scan rate, the potential values of

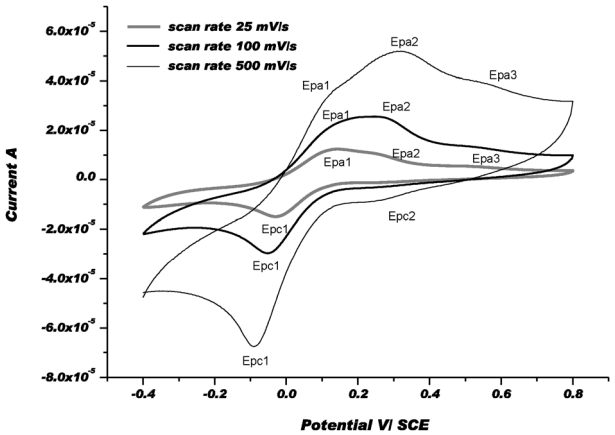

Fig. 11 CVs of $[Cu\mathbf{L8}(DMF)_2]^{2+}$ at 3 different scan rates: 25, 100, and 500 mV s^{-1} in Ar-purged DMF with Bu_4NPF_6 0.1 M as a supporting electrolyte at rt.

Epc1 were close to those summarised in Table 5. It was inferred that the chemical rearrangements after the electronic transfer may be easier and the chemical reaction constants associated with the chemical steps C_{ox} are faster in the more flexible acyclic series than in the cyclic series. However, one should notice that these systems can be almost totally reversed at scan rates below 100 mV s^{-1} and 25 mV s^{-1} in the acyclic series and cyclic series, respectively. Comparison of these results (for the acyclic and cyclic series) with those obtained by others with analogous mononuclear Cu(II) complexes coordinated by nitrogen or sulfur atoms in the ligands show that the Cu(II)/Cu(I) couples occur within about the same potential domain, between *ca.* −0.4 and −1.0 V *vs.* SCE.[54] However, chemical reorganisation steps inducing the formation of metastable intermediates, *i.e.* Cu(II)met and Cu(I)met, seem to be easier with diaza-crown ethers due to the weaker energy of the Cu–O bond than those of Cu–N or Cu–S bonds.[55] More than two conformational metastable intermediates are generated for both oxidized and reduced species, preceding or succeeding the electron transfer steps in diaza-crown ether copper(II) complexes. Finally, the global mechanism is likely more complicated than the classical square-scheme mechanism generally proposed for electron transfer in Cu(II)/Cu(I) systems. This may be attributed mainly to the weakness of the Cu–O bond strength by comparison to the Cu–N and Cu–S bond strengths. Altogether, the present electrochemical study shows that the electron-transfer process is accompanied by bond ruptures (or formations) and changes in reversible ligand conformation particularly in the acyclic series.

EPR measurements

Acyclic complexes (*i.e.* from ligands **L5–9**) will be discussed first as they displayed much more simple EPR-spectra than cyclic ones. The X-band EPR spectra of $[Cu\mathbf{L7}(MeCN)]^{2+}$ and $[Cu\mathbf{L8}(DMF)_2]^{2+}$ complexes recorded at 100 K in frozen DMF are presented in Fig. 12 together with simulations.

Fit parameters of acyclic complexes (see Table 6) are typical of a square-based coordination polyhedra[56] and characteristic

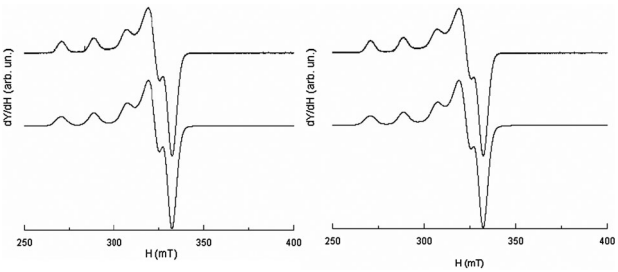

Fig. 12 EPR spectrum recorded at the X-band (10^{-3} M in DMF at 100 K) of $[Cu\mathbf{L7}(MeCN)]^{2+}$ (left) and $[Cu\mathbf{L8}(DMF)_2]^{2+}$ (right); experimental (upper traces), simulation (lower traces).

Table 6 Anisotropic EPR-spectral data of Cu(II)-complexes from acyclic ligands **L5–9** (10^{-3} M in DMF at 100 K)

	g Tensor		Hyperfine coupling tensor to ^{63}Cu		
Complex	$g_\perp$	$g_\parallel$	$A(Cu)_\perp$ 10^{-4} cm^{-1}	$A(Cu)_\parallel$ 10^{-4} cm^{-1}	$g_\parallel/A_\parallel$ cm
$[Cu\mathbf{L5}(MeCN)]^{2+}$	2.056	2.289 (~60%)	49	160	143
		2.220 (~40%)		163	136
$[Cu\mathbf{L6}(ClO_4)]^{+}$	2.054	2.233	14	183	122
$[Cu\mathbf{L7}(MeCN)]^{2+}$	2.058	2.234	12	186	120
$[Cu\mathbf{L8}(DMF)_2]^{2+}$	2.058	2.236	13	185	121
$[Cu\mathbf{L9}(ClO_4)]^{+}$	2.054	2.237	9	192	116

of a Cu(II)-ion coordinated with four N-nuclei within a planar (or near planar) configuration.[57]

Since EPR parameters may also reflect the degree of distortion of copper(II) complexes, the $g_\parallel/A_\parallel$ ratio is given as a rough estimate of coordination geometry. Values of 110–120 are reported as typical of 'planar' complexes while the range between 130–150 is characteristic of slight to moderate distortion and 180–250 indicates strong distortion.[58] Higher frequency, *e.g.* the Q-band EPR spectroscopy, is well known to facilitate the interpretation of intricate spectra where several interactions are intermingled.

Although the Q-band was not required to solve the geometry of $[Cu\mathbf{L6}(ClO_4)]^{+}$ (*i.e.* Fig. 13, right), it will serve as a reference for comparison with more complicated systems. It appears that the X-band and Q-band parameters for simulations are quite consistent with the geometry of the complex in the solid state. These parameters are also very similar to those of **L7** and **L8**

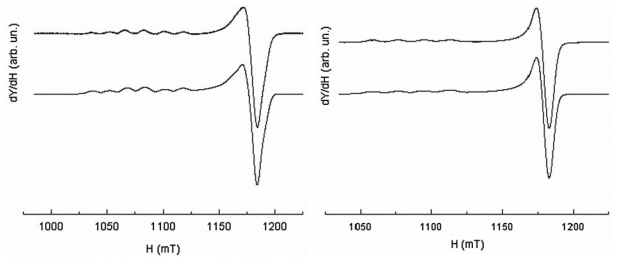

Fig. 13 EPR spectrum recorded at the Q-band and 100 K (10^{-3} M in DMF at 100 K) of $[Cu\mathbf{L5}(MeCN)]^{2+}$ (left) and $[Cu\mathbf{L6}(ClO_4)]^{+}$ (right); experimental (upper traces), simulation (lower traces).

Cu(II)-complexes. The parallel components of the EPR spectra of **L6**, **L7**, **L8**, and **L9** Cu(II)-complexes (see Table 6) confirm the rather undistorted 'planar' geometry in frozen solution consistent with their X-ray crystal structures. $[Cu\mathbf{L6}(ClO_4)]^+$ and $[Cu\mathbf{L7}(MeCN)]^{2+}$ do not show any significant difference in their EPR parameters despite the supplementary bond between the triazole and the phenyl ring in **L6** and their different coordination mode in the solid state. Yet, the Q-band EPR spectrum of $[Cu\mathbf{L5}(MeCN)]^{2+}$ in frozen solution (see Fig. 13, left) requires two components for a satisfactory fit with two slightly different values of $g_{\|}$. The major contribution (*ca.* 60%) points to an increasing axial character with an increase in $g_{\|}$ and a decrease in $A_{\|}$ as compared to $[Cu\mathbf{L7}(MeCN)]^{2+}$, $[Cu\mathbf{L8}(DMF)_2]^{2+}$, and $[Cu\mathbf{L9}(ClO_4)]^+$ complexes (see S1 in ESI†). Concerning $[Cu\mathbf{L5}(MeCN)]^{2+}$, the higher value of $g_{\|}/A_{\|}$ is indicative of a moderate distortion in agreement with its crystalline structure which might correspond to the more stable conformer in DMF at 100 K.[59] In the cyclic series, the Q-band spectra of $[Cu\mathbf{L3}]^{2+}$ and $[Cu\mathbf{L4}]^{2+}$ are similar in frozen solution (see Fig. 14, left part for experimental and simulation spectra of $[Cu\mathbf{L3}]^{2+}$ and ESI† S2 for $[Cu\mathbf{L4}]^{2+}$). Such signals are characteristic of a mixture of binuclear species, that means species in which two close copper nuclei interact *via* an intermolecular way, and mononuclear copper species.[60–63] Fig. 14's right part illustrates the component positions of tensor **g** (g_x, g_y and g_z) of binuclear species with the zero-field splitting D and the hyperfine contribution A_z for two equivalent copper nuclei. The index $_{\|}$ or $_{\perp}$ is related to the mononuclear complex. Please, note that $A_{\|}$ is roughly twice as high as A_z in agreement with the delocalization of the electronic cloud over two copper nuclei. The value of 2D was assessed from the splitting of copper parallel lines (180 G). Within the point-dipole approximation, it corresponds to a r_{Cu-Cu} spin–spin distance of *ca.* 5.9 Å.

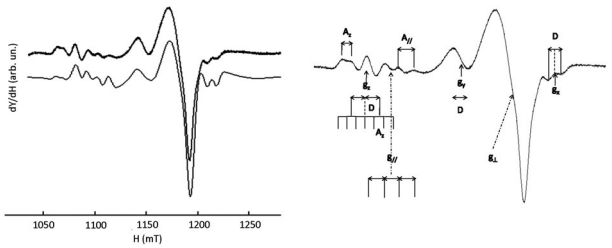

Fig. 14 EPR spectrum of $[Cu\mathbf{L3}]^{2+}$ recorded at the Q-band (10^{-3} M in DMF at 100 K); left: experimental (upper trace), simulation (lower trace); right: visualization of the EPR features associated with the di-nuclear complex (S = 1) labelled *x*, *y*, and *z* and with the mono-nuclear complex (S = 1/2) labelled $_{\|}$ and $_{\perp}$.

Table 7 Anisotropic EPR-spectral data of $[Cu\mathbf{L3}]^{2+}$ (10^{-3} M in DMF at 100 K)

S = 1 (dinuclear species, weight: 17%)				
g_z	g_y	g_x	A_z (10^{-4} cm^{-1})	D (10^{-4} cm^{-1})
2.250	2.115	2.003	65	84
S = 1/2 (mononuclear complex, weight: 83%)				
$g_{\|}$	$g_{\perp}$		$A_{\|}$ (10^{-4} cm^{-1})	$g_{\|}/A_{\|}$
2.214	2.061	2.039	107	207

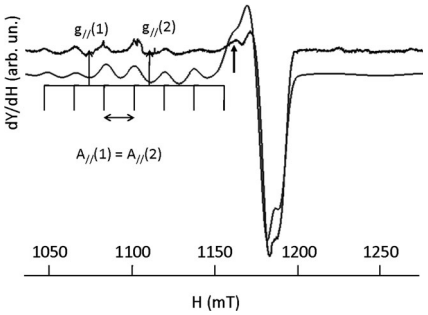

Fig. 15 EPR spectrum of $[Cu\mathbf{L2}]^{2+}$ recorded at the Q-band (10^{-3} M in DMF at 100 K) experimental (upper trace), simulation (lower trace).

Table 8 Anisotropic EPR-spectral data of $[Cu\mathbf{L2}]^{2+}$ (10^{-3} M in DMF at 100 K)

S = 1/2 (mononuclear complex, weight: 37%)			
$g_{\|}$	$g_{\perp}$	$A_{\|}$ (10^{-4} cm^{-1})	$g_{\|}/A_{\|}$
2.258	2.045	177	127
S = 1/2 (mononuclear complex, weight: 63%)			
$g_{\|}$	$g_{\perp}$	$A_{\|}$ (10^{-4} cm^{-1})	$g_{\|}/A_{\|}$
2.182	2.061	177	123

The EPR data of mononuclear and dinuclear complexes of $[Cu\mathbf{L3}]^{2+}$ in Table 7 were obtained by simulation of the entire spectrum.

The $g_{\|}/A_{\|}$ ratio is high compared to the acyclic complexes as expected for a more distorted environment of the metal ion.[59] The Q-band spectrum of $[Cu\mathbf{L2}]^{2+}$ (*vide infra* Fig. 15) results from the superimposition of two mononuclear species with very low dipolar interaction between them as revealed by a weak peak at 1163 mT (→). Such a faint contribution is not visible on the parallel part of the spectrum. Indeed, all peaks in the low field zone are equidistant.

EPR data for the $[Cu\mathbf{L2}]^{2+}$ complex are summarized in Table 8.

A tentative explanation is these solutions contain at 100 K a mixture of two more or less distorted structural species (*i.e.* conformers) one of them promoting the formation of dimeric species. The number and kind of bonds, and the so-called 'crown effect', obviously influence the flexibility and the stability of such complexes in DMF, especially at low temperatures.[59,62]

Conclusion

Novel ligands bearing two 1,4-substituted-triazole moieties as coordinating side-arms (*i.e.* **L2–9**) were easily prepared in one step from two commercial *N*,*N*′-dimethyl-alkyl diamines or from a known C_2-symmetric *N*,*N*′-dipropargyl-diaza-18-crown-6 *via* the Cu(I)-catalyzed Huisgen dipolar cycloaddition. Changing the alkyl-substituent of the azide (*i.e.* benzyl, phenyl, *p*-methoxy- or *p*-chloro-phenyl) gave access to stable mononuclear Cu(II)-complexes with different geometries and coordinations in the solid state. Their electrochemical studies proved that the electron transfer induces intricate but reversible reorganisation of

the cation coordination shell with a first cathodic peak varying within a maximum 0.16 V range. The EPR-spectrum of cyclic $[Cu\mathbf{L2}]^{2+}$, $[Cu\mathbf{L3}]^{2+}$ & $[Cu\mathbf{L4}]^{2+}$ – and to a smaller extent that of $[Cu\mathbf{L5}(MeCN)]^{2+}$ – exhibited two mononuclear species (or conformers) signals in frozen DMF at 100 K, one of them promoting the formation of dinuclear species as a minor component. Altogether these behaviours suggest that such complexes could be proposed as catalysts (*e.g.* for the oxidation of alcohols in carbonyl compounds or as artificial enzymes).[64] Lastly, the cytotoxicity of some of these complexes towards uterine human sarcoma cells was investigated and showed promising activities.[65]

Experimental section

Chemicals and solvents (reagent grade or better) were purchased from Sigma-Aldrich except spectrophotometric-grade DMF which was purchased from Alfa-Aesar [ref. 13808]. Anhydrous solvents were dried by usual procedures and stored over 4 Å molecular sieves under Ar before use. Chromatography was carried out using Grace silicagel (Davisil® LC60A 70–200 μm) or basic Al_2O_3 when stated (Sigma-Aldrich ref. 199443). ^{1}H & ^{13}C-NMR spectra were recorded on a Bruker AC250 spectrometer at 250 MHz for ^{1}H and 62.9 MHz for ^{13}C in $CDCl_3$ if no other conditions are stated. Chemical shifts δ were measured with respect to the CH_3CN signal (2.10 ppm for ^{1}H and 1.89 ppm for ^{13}C-NMR). CHN elemental analyses were performed using a Thermo Finnigan EA 1112 Series Flash Elemental Analyzer. ES$^+$-HRMS spectra were obtained using a Bruker micrOTOFq mass spectrometer with capillary tensions between −1200 and −4500 V from diluted MeCN solutions. FT-IR spectra were obtained from KBr-pellets (if not other stated) on a Perkin Elmer Spectrum 1000 spectrophotometer. UV-visible spectra were recorded on a Perkin-Elmer Lambda1050 UV-Vis-NIR spectrophotometer using a 1 cm-optical-pathlength cell at T = 298 K. X-ray structures were determined using a Bruker-Nonius Kappa APEXII or a Agilent SuperNova diffractometer equipped with a low temperature device using liquid N_2 to perform XRD intensity measurements near 100 K. X-ray source was a sealed tube giving Mo Kα radiation (λ = 0.71073 Å). Diffraction pattern frames were processed with Apex or CrysAlis software. The structures were solved by direct methods using the SIR software package[66a] and refined by full matrix least-squares on F squared using SHELXL software.[66b] In both crystal structure models, non-hydrogen atoms were located in the difference Fourier syntheses and were refined with anisotropic thermal parameters. Observed hydrogen atoms were placed at calculated positions using a riding model. Cyclic voltammetry (CV) was performed using a Radiometer PST006 potentiostat using a conventional three-electrode cell at rt. The KCl calomel electrode (SCE) was separated from the test compartment using a bridge tube. The test solution was dimethylformamide containing 10^{-1} M tetrabutylammonium hexafluorophosphate as the supporting electrolyte. The working electrode was a 10 mm Pt wire and the counter-electrode a 1 cm^2 vitreous carbon disc. 5.0×10^{-4} M fresh solution of each studied compound was used and purged for 5 min with Ar before each measurement. All potentials were quoted *versus* SCE. Under these conditions the redox potential of the couple Fc^+/Fc was found to be 0.47 V. EPR spectra were recorded using a continuous-wave EMXplus spectrometer (Bruker Biospin GmbH, Germany) equipped with a high sensitivity resonator (4119HS-W1, Bruker). The spectrometer was tuned such that settings (modulation coils, incident microwave power) were not distorting the EPR signal (X-band Larmor frequency ∼9.3 GHz and Q-band Larmor frequency ∼34 GHz). Measurements were carried out in frozen 10^{-3} M DMF (ACS reagent ≥ 99.8% GC) solutions of copper(II) complexes held at 100 K with liquid nitrogen. Simulations were generated with the EasySpin free software.[67]

General procedure I

Synthesis of ligands **L2–4**. To a stirred suspension of *N*,*N*′-bis-propargyl-diaza-18-6 crown ether A[49] (500 mg, 1.47 mmol) in a mixture of water–acetonitrile (1 : 1, 25 mL) at rt were added the aryl-azide (2.1 eq.), Na-ascorbate (117 mg, 0.4 eq.), and $CuSO_4 \cdot 5H_2O$ (74 mg, 0.2 eq.) under Ar. The resulting brownish solution was stirred overnight at rt under Ar. The reaction mixture was filtered, extracted with CH_2Cl_2 (4 × 90 mL), and the organic phases were combined, washed with 5% aq. NH_4OH (2 × 20 mL), brine (20 mL), water (3 × 20 mL), dried over $MgSO_4$, and finally evaporated under reduced pressure. The crude material was purified by liquid chromatography on silica (and/or alumina) with mixtures of CH_2Cl_2–MeOH as eluents.

General procedure II

Synthesis of ligands **L5–9**. A solution of symmetric sec. *N*,*N*′-dimethylamine (B or C, 5.0 mmol), triethylamine (1.5 mL, 2.15 eq.), and propargyl bromide (80 wt% in toluene, 1.2 mL, 2.15 eq.) in a mixture of acetonitrile–water (1 : 1, 90 mL) was stirred for 90 min at rt under Ar. The organic azide (2.15 eq.), Na-ascorbate (0.4 g, 0.4 eq.), and $CuSO_4 \cdot 5H_2O$ (0.25 g, 0.2 eq.) were then added and the resulting brownish solution was stirred overnight at rt under Ar. The reaction mixture was filtered on a sintered glass, extracted with CH_2Cl_2 (4 × 90 mL), and the organic phases were combined, washed with 5% aq. NH_4OH (2 × 20 mL), brine (20 mL), water (3 × 20 mL), dried over $MgSO_4$, and finally evaporated under reduced pressure. The crude resulting gum was purified by liquid chromatography (LC) on silica or alumina with mixtures of CH_2Cl_2–MeOH as eluents.

General procedure III

Synthesis of Cu-complexes. **Warning: perchlorates are potentially explosive compounds. While we have experienced no problems during our syntheses, extreme care must be taken when working with perchlorate complexes or salts and only small quantities should be handled!** $Cu(ClO_4)_2 \cdot 6H_2O$ (1.2 eq.) was dissolved in a solution of the ligand (50.0 mg) in a mixture of acetonitrile–water–EtOH (3 mL, 1 : 1 : 1) at rt. The resulting suspension was stirred for 2 h at 70 °C, allowed to cool to rt, filtered through a small cotton pad, concentrated to half, diluted with two drops of DMF (*ca.* 30 mg), and finally stored for several days in the dark at 4 °C. Crystallographic-suitable

monocrystals were isolated by filtration on a sintered glass, rinsed with dist. H_2O, CH_2Cl_2, and finally dried at rt in the dark.

Acknowledgements

M. A. gratefully acknowledges financial support from the French National Research Agency *via* a post-doctoral grant (ANR-09-BLAN-0180-01). The authors warmly thank the 'Institut Jean Barriol' for X-ray diffraction measurement facilities and Dr Slimane Dahaoui (radio-crystallographic measurements and structure determination), Mr François Dupire for measuring HRMS, Mr Stéphane Parant for recording UV-Vis and Mrs Sandrine Adach for performing elemental analysis.

Notes and references

1 D. B. Rorabacher, *Chem. Rev.*, 2004, **104**, 651–697.
2 G. C. M. Steffens, R. Biewald and G. Buse, *Eur. J. Biochem.*, 1987, **164**, 295–300.
3 C. F. Wright, D. H. Hamer and K. McKenney, *J. Biol. Chem.*, 1988, **263**, 1570–1574.
4 B. S. Magdoff-Fairchild, F. M. Lovell and B. W. Low, *J. Biol. Chem.*, 1969, **244**, 3497–3499.
5 S. S. Hasnain, G. P. Diakun, P. F. Knowles, N. Binsted, C. D. Garner and N. J. Blackburn, *Biochem. J.*, 1984, **221**, 545–548.
6 F. Thomas, *Eur. J. Inorg. Chem.*, 2007, 2379–2404.
7 V. Desai and S. G. Kaler, *Am. J. Clin. Nutr.*, 2008, **88**, 855S–858S.
8 W. Kaim and J. Rall, *Angew. Chem., Int. Ed. Engl.*, 1996, **35**, 43–60.
9 J. Nelson, *Annu. Rep. Prog. Chem., Sect. A: Inorg. Chem.*, 2010, **106**, 235–254.
10 C. J. Fritchie, *J. Biol. Chem.*, 1973, **248**, 7516–7521.
11 I. A. Koval, K. Selmeczi, C. Belle, C. Philouze, E. Saint-Aman, I. Gautier-Luneau, A. M. Schuitema, M. van Vliet, P. Gamez, O. Roubeau, M. Lüken, B. Krebs, M. Lutz, A. L. Spek, J.-L. Pierre and J. Reedijk, *Chem.–Eur. J.*, 2006, **12**, 6138–6150.
12 A. L. Abuhijleh and J. Khalaf, *Eur. J. Med. Chem.*, 2010, **45**, 3811–3817.
13 S. García-Gallego, M. J. Serramía, E. Arnaiz, L. Díaz, M. A. Muñoz-Fernández, P. Gómez-Sal, M. F. Ottaviani, R. Gómez and F. J. de la Mata, *Eur. J. Inorg. Chem.*, 2011, 1657–1665.
14 B. S. Creaven, B. Duff, D. A. Egan, K. Kavanagh, G. Rosair, T. Thangella, R. Venkat and M. Walsh, *Inorg. Chim. Acta*, 2010, **363**, 4048–4058.
15 E. N. da Silva Jr, M. A. B. F. de Moura, A. V. Pinto, M. C. F. R. Pinto, M. C. B. V. de Souza, A. J. Araújo, C. Pessoa, L. V. Costa-Lotufo, R. C. Montenegro, M. O. de Moraes, V. F. Ferreir and M. O. F. Goulart, *J. Braz. Chem. Soc.*, 2009, **20**, 635–643.
16 O. Jacobson, I. D. Weiss, L. Szajek, J. M. Farber and D. O. Kiesewetter, *Bioorg. Med. Chem.*, 2009, **17**, 1486–1493.
17 M. Shokeen and T. J. Wadas, *Med. Chem.*, 2011, **7**, 413–429.
18 E. Hao, Z. Wang, L. Jiao and S. Wang, *Dalton Trans.*, 2010, **39**, 2660–2666.
19 J. Xiang, Y.-G. Yin and P. Mei, *Inorg. Chem. Commun.*, 2007, **10**, 1168–1171.
20 P. S. Donnelly, S. D. Zanatta, S. C. Zammit, J. M. White and S. J. Williams, *Chem. Commun.*, 2008, 2459–2461.
21 T. L. Mindt, C. Schweinsberg, L. Brans, A. Hagenbach, U. Abram, D. Tourwé, E. Garcia-Garayoa and R. Schibli, *ChemMedChem*, 2009, **4**, 529–539.
22 G. F. Manbeck, W. W. Brennessel and R. Eisenberg, *Inorg. Chem.*, 2011, **50**, 3431–3441.
23 C. B. Anderson, B. Christopher, A. B. S. Elliott, J. E. M. Lewis, C. J. McAdam, K. C. Gordon and J. D. Crowley, *Dalton Trans.*, 2012, **41**, 14625–14632.
24 W. Yang and Y. Zhong, *Chin. J. Chem.*, 2013, **31**, 329–338.
25 C. B. Anderson, A. B. S. Elliott, C. J. McAdam, K. C. Gordon and J. D. Crowley, *Organometallics*, 2013, **32**, 788–797.
26 D. Wang, D. Denux, J. Ruiz and D. Astruc, *Adv. Synth. Catal.*, 2013, **355**, 129–142.
27 J. M. Fernandez-Hernandez, J. I. Beltran, V. Lemaur, M.-D. Galvez-Lopez, C.-H. Chien, F. Polo, E. Orselli, R. Froehlich, J. Cornil and L. De Cola, *Inorg. Chem.*, 2013, **52**, 1812–1824; and literature cited therein.
28 B. M. J. M. Suijkerbuijk, B. N. H. Aerts, H. P. Dijkstra, M. Lutz, A. L. Spek, G. van Koten and R. J. M. Klein Gebbink, *Dalton Trans.*, 2007, 1273–1276.
29 J. D. Crowley and D. A. McMorran, *Top. Heterocycl. Chem.*, 2012, **28**, 31–84.
30 P.-Y. Jin, P. Jin, Y.-A. Ruan, Y. Ju and Y.-F. Zhao, *Synlett*, 2007, 3003–3006.
31 G. E. Kostatis, P. Xydias, E. Nordlander and J. C. Plakatouras, *Inorg. Chim. Acta*, 2012, **383**, 327–331.
32 R. Huisgen, G. Szeimies and L. Mœbius, *Chem. Ber.*, 1967, **100**, 2494–2507.
33 J. Bastide, J. Hamelin, F. Texier and Y. Vo Quang, *Bull. Soc. Chim. Fr.*, 1973, **7–8**, 555–2579.
34 R. Huisgen, *Pure Appl. Chem.*, 1989, **61**, 613–628.
35 Q. Wang, S. Chittaboina and H. N. Barnhill, *Lett. Org. Chem.*, 2005, **2**, 293–301.
36 H. C. Kolb, M. G. Finn and K. B. Sharpless, *Angew. Chem.*, 2001, **113**, 2056–2075.
37 V. V. Rostovtsev, L. G. Green, V. V. Fokin and K. B. Sharpless, *Angew. Chem.*, 2002, **114**, 2708–2711.
38 C. W. Tornøe, C. Christensen and M. Meldal, *J. Org. Chem.*, 2002, **67**, 3057–3064.
39 H. Struthers, T. L. Mindt and R. Schibli, *Dalton Trans.*, 2010, **39**, 675–696.
40 E. Tamanini, A. Katewa, L. M. Sedger, M. H. Todd and M. Watkinson, *Inorg. Chem.*, 2009, **48**, 319–324.
41 E. Tamanini, K. Flavin, M. Motevalli, S. Piperno, L. A. Gheber, M. H. Todd and M. Watkinson, *Inorg. Chem.*, 2010, **49**, 3789–3800.
42 L.-D. Li, C. S. B. Gomes, P. T. Gomes and M. T. Duarte, *Dalton Trans.*, 2011, **40**, 3365–3380.
43 A. Späth, E.-M. Rummel and B. König, *Molbank*, 2010, M663.
44 Z. Jia, R. K. Singh and D. Wang, Biomedical Applications of ''Click''-Modified Cyclodextrins, in *Click Chemistry in*

Glycoscience: New Developments and Strategies, ed. Z. J. Witczak and R. Bielski, John Wiley & Sons, Inc., 2013, ch. 11.
45 J.-P. Joly, M. Beley, K. Selmeczi and E. Wenger, *Inorg. Chem. Commun.*, 2009, **12**, 382–384.
46 Submitted for publication.
47 V. J. Gatto, K. A. Arnold, A. M. Viscariello, S. R. Miller, C. R. Morgan and G. W. Gokel, *J. Org. Chem.*, 1986, **51**, 5373–5384.
48 F. Moulin, *Helv. Chim. Acta*, 1952, **35**, 167–180.
49 I. Wilkening, G. del Signore and C. P. R. Hackenberger, *Chem. Commun.*, 2010, **47**, 349–351.
50 A. Zarei, A. R. Hajipour, L. Khazdooz and H. Aghaei, *Tetrahedron Lett.*, 2009, **50**, 4443–4445.
51 Z.-Y. Yan, Y.-B. Zhao, M.-J. Fan, W.-M. Liu and Y.-M. Liang, *Tetrahedron*, 2005, **61**, 9331–9337.
52 M. V. Veidis, G. H. Schreiber, T. E. Gough and G. J. Palenik, *J. Am. Chem. Soc.*, 1969, **91**, 1859–1860.
53 F.-Y. Dong, Y.-T. Li, Z.-Y. Wu, J.-M. Dou and D.-Q. Wang, *J. Chem. Crystallogr.*, 2007, **37**, 445–449.
54 A. Cheansirisomboon, S. Youngme, C. Pakawatchai and N. Chaichit, *Mendeleev Commun.*, 2010, **20**, 109–110.
55 N. M. Villeneuve, R. R. Schroeder, L. A. Ochrymowycz and D. B. Rorabacher, *Inorg. Chem.*, 1997, **36**, 4475–4483.
56 E. V. Rybak-Akimova, A. Y. Nazarenko, L. Chen, P. W. Krieger, A. M. Herrera, V. V. Tarasov and P. D. Robinson, *Inorg. Chim. Acta*, 2001, **324**, 1–15.
57 E. Tamari, S. E. J. Rigby, M. Motevalli, M. H. Todd and M. Watkinson, *Chem.–Eur. J.*, 2009, **15**, 3720–3728.
58 A. W. Addison, Spectroscopic and redox trends from model copper complexes, in *Copper Coordination Chemistry: Biochemical and Inorganic Perspectives*, ed. K. D. Karlin and J. Zubieta, Adenine Press, New York, 1983.
59 V. C. da Silveira, G. F. Caramori, M. P. Abbott, M. B. Gonçalves, H. M. Petrilli and A. M. da Costa Ferreira, *J. Inorg. Biochem.*, 2009, **103**, 1331–1341.
60 S. S. Eaton, G. R. Eaton and C. K. Chang, *J. Am. Chem. Soc.*, 1985, **107**, 3177–3184.
61 L. J. Singh, N. S. Devi, S. P. Devi, W. B. Devi, R. K. Hemakumar Singh, B. Rajeswari and R. M. Kadam, *Inorg. Chem. Commun*, 2010, **13**, 365–368.
62 D. da G. J. Batista, P. B. da Silva, L. Stivanin, D. R. Lachter, R. S. Silva, J. Felcman, S. R. W. Louro, L. R. Teixeira, M. de Nazaré and C. Soeiro, *Polyhedron*, 2011, **30**, 1718–1725.
63 J. A. Weil and J. R. Bolton, in *Electron Paramagnetic Resonance, Elementary Theory and Practical Applications*, ed. J. A. Weil and J. R. Bolton, John Wiley & Sons, Inc., 1993, ch. 6.3.
64 F. Rosati and G. Roelfes, *ChemCatChem*, 2010, **2**, 916–927.
65 Q. A. De Paula, J.-P. Joly, K. Selmeczi, P. Colepicolo, G. Indig, A. M. Da Costa Ferreira, Eurobic 11 – Granada (Spain) Sept. 12–16, 2012.
66 (*a*) A. Altomare, M. C. Burla, M. Camalli, G. L. Cascarano, C. Giacovazzo, A. Guagliardi, A. G. G. Moliterni, G. Polidori and G. Spagna, *J. Appl. Crystallogr.*, 1999, **32**, 115–119; (*b*) G. M. Sheldrick, *SHELXS97 and SHELXL97*, University of Göttingen, Germany, 1997.
67 S. Stoll and A. Schweiger, *J. Magn. Reson.*, 2006, **178**, 42–55.